isvr Institute of Sound and Vibration Research

Analytical Study of Pantograph-Catenary System Dynamics

T.X. Wu and M.J. Brennan

ISVR Technical Memorandum 819

June 1997

University of Southampton

SCIENTIFIC PUBLICATIONS BY THE ISVR

Technical Reports are published to promote timely dissemination of research results by ISVR personnel. This medium permits more detailed presentation than is usually acceptable for scientific journals. Responsibility for both the content and any opinions expressed rests entirely with the author(s).

Technical Memoranda are produced to enable the early or preliminary release of information by ISVR personnel where such release is deemed to the appropriate. Information contained in these memoranda may be incomplete, or form part of a continuing programme; this should be borne in mind when using or quoting from these documents.

Contract Reports are produced to record the results of scientific work carried out for sponsors, under contract. The ISVR treats these reports as confidential to sponsors and does not make them available for general circulation. Individual sponsors may, however, authorize subsequent release of the material.

UNIVERSITY OF SOUTHAMPTON

INSTITUTE OF SOUND AND VIBRATION RESEARCH

STRUCTURAL DYNAMICS GROUP

Analytical Study of Pantograph-Catenary System Dynamics

by

T.X. Wu and M.J. Brennan

ISVR Technical Memorandum No. 819

June 1997

Authorized for issue by
Dr. R.J. Pinnington
Group Chairman

TABLE OF CONTENTS

		Page No.
	LIST OF FIGURES	
	ABSTRACT	
1.	INTRODUCTION	
2.		
3.	AN ACTIVE PANTOGRAPH	
	3.1 Open-loop control	6
	3.2 Feedback control	10
	3.3 Optimal feedback control	12
4.	CONCLUSION	15
5.	REFERENCES	17
6.	FIGURES	19

LIST OF FIGURES

Figure 1 Pantograph and overhead wire.

Figure 2 Catenary system: (a) Heavy compound catenary; (b) Simple catenary.

Figure 3 Discretization of catenary.

Figure 4 Stiffness of contact wire in a span: (a) $T_1 = 24.5$ kN, $T_2 = T_3 = 14.7$ kN; (b) $T_1 = T_3 = 14.7$ kN, $T_2 = 24.5$ kN; (c) $T_1 = T_2 = 14.7$ kN, $T_3 = 24.5$ kN; (d) $T_1 = T_2 = 9.8$ kN.

Figure 5 Pantograph model.

Figure 6 Model of pantograph-catenary system.

Figure 7 Stable and unstable regions of pantograph-catenary system: — $\zeta = 0$; ····· $\zeta = 0.01$; – – – $\zeta = 0.02$.

Figure 8 Comparison between solutions by numerical method and perturbation method: — the 4th Runge-Kutta method; ····· perturbation method.

Figure 9 Peak-to-peak and maximum displacement, $\zeta = 0.05$ and $f = 1$: — peak-to-peak displacement; – · – · maximum displacement. (a) $\alpha = 0.3$, (b) $\alpha = 0.4$, (c) $\alpha = 0.5$, (d) $\alpha = 0.6$.

Figure 10 Peak-to-peak and maximum contact force, $\zeta = 0.05$ and $f = 1$: — peak-to-peak contact force; – · – · maximum contact force. (a) $\alpha = 0.3$, (b) $\alpha = 0.4$, (c) $\alpha = 0.5$, (d) $\alpha = 0.6$.

Figure 11 Peak-to-peak and maximum displacement, $\zeta = 0.1$ and $f = 1$: — peak-to-peak displacement; – · – · maximum displacement. (a) $\alpha = 0.3$, (b) $\alpha = 0.4$, (c) $\alpha = 0.5$, (d) $\alpha = 0.6$.

Figure 12 Peak-to-peak and maximum contact force, $\zeta = 0.1$ and $f = 1$:
— peak-to-peak contact force; – · – · maximum contact force.
(a) $\alpha = 0.3$, (b) $\alpha = 0.4$, (c) $\alpha = 0.5$, (d) $\alpha = 0.6$.

Figure 13 Two DOF model of pantograph-catenary system.

Figure 14 Comparison of the steady-state response from the two DOF model and SDOF model at v = 300 km/h: — SDOF model; – – – two DOF model with $K_1 = 39000$ N/m; ····· two DOF model with $K_1 = 20000$ N/m.

Figure 15 Influences of different mass with $K_1 = 39000$ N/m, $C_1 = 120$ Ns/m and $C_2 = 30$ Ns/m: — $M_1 = 6.5$ kg, $M_2 = 8.5$ kg, ····· $M_1 = 4.0$ kg, $M_2 = 8.5$ kg, – – – $M_1 = 6.5$ kg, $M_2 = 6.0$ kg.

Figure 16 Influences of different stiffness between head and frame with $M_1 = 6.5$ kg, $M_2 = 8.5$ kg, $C_1 = 120$ Ns/m and $C_2 = 30$ Ns/m: — $K_1 = 39000$ N/m, – – – $K_1 = 20000$ N/m, ····· $K_1 = 10000$ N/m.

ABSTRACT

For a high speed electrical rail system, good dynamic performance of the pantograph-catenary system is vital for smooth and continuous current collection. To facilitate the prediction of the dynamic behaviour of the pantograph-catenary system, a periodically time-varying SDOF model is developed in this paper which allows an analytical approach to the solution of the system. The stabilities of the pantograph-catenary system are investigated, and both the displacement of the pantograph head and the contact force between the pantograph head and the overhead wire are calculated. The model used in this paper shows that the vibration of the pantograph is not caused by an instability, but is parametrically excited by the variable stiffness of the catenary. To reduce the variation in the contact force and hence improve the current collection either the mass of the pantograph head should be reduced, or the average stiffness of the catenary should be increased.

1. INTRODUCTION

High speed electric rail is competitive with airlines for journeys between several hundred and one thousand kilometres if the operational speed of trains can reach around 250 kilometres per hour or greater. One of the main problems to be solved for high speed electric rail is the power supply. Electric trains derive power from an overhead contact wire system (catenary), and current collection is accomplished through a pantograph mechanism mounted on the roof of the locomotive. A picture showing this arrangement is shown in Figure 1. Unfortunately, as the speed of a train increases, the variation in contact force between the pantograph head and contact wire also increases, which can lead to a loss of contact, arcing and wear.

The pantograph-catenary combination is a dynamic coupled system. This means the dynamic response of the catenary affects that of the pantograph and vice versa. To achieve a better understanding of the pantograph-catenary system's dynamic behaviour much research work has been done over the years using various techniques. An approximate analytical solution for the contact force was presented by Ockendon *et al* [1]. Vinayagaligam [2] studied the variation of this force and the panhead trajectory by using the finite difference method. Wormley *et al* [3] obtained the free vibration modes of the overhead wire system and the contact force by using the Rayleigh-Ritz and modal analysis methods. A non-linear, lumped parameter pantograph model has been developed by Seering *et al* [4] to simulate its dynamic performance, and this was compared with experimental data. Wu [5] established a finite element model of the overhead wire system to determine its initial state, static stiffness variation and natural frequencies and modes. Using this FE model combined with a lumped pantograph model, the current collection problem was studied by Wu [6]. Manabe [7] studied the dynamic response of the overhead wire, and the energy propagation in the wire by using a model of a stable load travelling along an infinite wire supported by discrete springs. Yagi *et al* [8] investigated the

dynamic response of the pantograph-catenary system to the lateral movement of the contact wire due to its zigzag layout.

Although different aspects of the system's dynamics have been studied and have produced valuable results, a clear and comprehensive description of the pantograph-catenary coupled system has not been reported so far. One of the main sources that cause the vibration of this system is the stiffness variation of the overhead wire along the span. In the middle of a span the stiffness of the overhead wire is minimum and near the support tower it is maximum. When the pantograph moves along the overhead wire, this stiffness variation produces a periodic excitation to the pantograph and leads to the vibration of the pantograph and the fluctuation of the contact force. On the other hand, when the panhead moves along the overhead wire, it causes flexural wave motion in the wire. In turn, this flexural wave propagation affects the contact force and the motion of the pantograph as well. This latter phenomenon is not discussed in this paper, because the primary aim of the paper is to investigate the effects of the time-varying stiffness of the catenary on the motion of the pantograph.

Thus, a simple mathematical model of the pantograph-catenary system which includes the main dynamic behaviour of the system is developed. It is simple enough to obtain an analytical solution to the problem which allows physical insight into the dynamic performance of the coupled system. The aims of the analytical approach are to study the basic dynamic properties of the pantograph-catenary system and to investigate the effects of the stiffness fluctuation of the overhead wire on the interaction between the overhead wire and the pantograph. Therefore, some factors such as excitation of the locomotive roof from below and aerodynamic forces on the pantograph have not been considered.

A FE method (FEM) is used to analyse the stiffness distributions of different types of catenary system. These are then coupled to linear models of the pantograph. A periodically time-varying single degree of freedom (SDOF) model is developed to describe the pantograph-catenary system's basic dynamic properties. This model is first used to examine the instabilities of the pantograph-catenary system, and then both the displacement of the pantograph head and the contact force are calculated using perturbation methods. Finally, a two DOF model is set up to simulate the pantograph-catenary system. A numerical method is used to investigate the behaviour of this system and the results are compared with those from the SDOF model to validate the simple model. Furthermore, the influences of some system parameters such as pantograph mass and damping, and the stiffness between the pantograph head and frame are also investigated.

The methods and results of this paper can be used to analyse existing pantograph-catenary systems and predict their dynamic performance. They also provide a theoretical framework for investigating improvements in the system design, and could be useful in the study of an active pantograph system.

2. ANALYSIS OF THE CATENARY SYSTEM

The overhead line systems shown in Fig. 2 are complicated systems which consist of two or three catenaries connected by some droppers which are fitted to minimise the droop of the contact wire. Because the catenary system is complex it is appropriate to calculate the stiffness of the contact wire using FEM [5]. For the coupled vibration of the pantograph-catenary system, the most important consideration is the stiffness variation of the contact wire in a span, because it is a primary source of vibration of the pantograph.

2.1 Stiffness matrix of a single catenary

The discretization of a continuous catenary is shown in Fig. 3. For simplicity every element is assumed to be the same length. The external force, including the weight of an element, is concentrated at the nodes. If the element is short enough, it can be considered to be a straight line, so the force balance equations at the nodes are

$$H\frac{y_2 - y_1}{\Delta x} - H\frac{y_1}{\Delta x} + f_1 = 0$$

$$H\frac{y_{i+1} - y_i}{\Delta x} - H\frac{y_i - y_{i-1}}{\Delta x} + f_i = 0 \qquad i = 2, 3, \ldots, n-1$$

$$H\frac{-y_n}{\Delta x} - H\frac{y_n - y_{n-1}}{\Delta x} + f_n = 0 \qquad (1a, b, c)$$

where H is the horizontal component of catenary tension, T, and $H \approx T$ when the droop of the catenary is small.

Equations (1a,b,c) can be represented in matrix form as

$$\mathbf{K_S Y_S} = \mathbf{F_S} \qquad (2)$$

where $\mathbf{K_S}$ is the stiffness matrix of the single catenary, $\mathbf{Y_S}$ is the vector of nodal displacements and $\mathbf{F_S}$ is the vector of vertical nodal forces. $\mathbf{K_S}$ is symmetric and its elements are given by:

$$k_{ii} = 2H/\Delta x \qquad i = 1, 2, \ldots, n$$

$$k_{i+1,i} = k_{i,i+1} = -H/\Delta x \qquad i = 1, 2, \ldots, n-1 \qquad (3a, b)$$

2.2 Stiffness matrix of the catenary system

The catenary system's stiffness matrix is composed of the catenary's stiffness matrix, $\mathbf{K}_c$, and the dropper's stiffness matrix, $\mathbf{K}_d$:

$$\mathbf{K} = \mathbf{K}_c + \mathbf{K}_d \tag{4}$$

where $\mathbf{K}_c$ has the form of

$$\begin{bmatrix} \mathbf{K}_{s1} & & & \\ & \mathbf{K}_{s2} & & \\ & & \ddots & \\ & & & \mathbf{K}_{sp} \end{bmatrix} \tag{5}$$

where $\mathbf{K}_{s1}, \mathbf{K}_{s2} \cdots \mathbf{K}_{sp}$ represent single catenary stiffness matrices which can be calculated using (3). $\mathbf{K}_d$ has the form,

$$\mathbf{K}_d = \sum_{m=1}^{M} \mathbf{K}_{dm} = \sum_{m=1}^{M} \begin{bmatrix} \ddots & & & \\ & k_m & \cdots & -k_m \\ & \vdots & \ddots & \vdots \\ & -k_m & \cdots & k_m \\ & & & \ddots \end{bmatrix} \begin{matrix} \\ \text{rth row} \\ \\ \text{sth row} \\ \\ \end{matrix} \tag{6}$$

$$\begin{matrix} & \text{rth} & \text{sth} \\ & \text{column} & \text{column} \end{matrix}$$

where $\mathbf{K}_{dm}$ is the matrix of a single dropper which is decided by the mth dropper's axial stiffness coefficient, k_m, and its two end positions, node r and node s.

2.3 Stiffness fluctuation of the contact wire in a span

To determine the stiffnesses of the catenary system we apply a force, f_i, to node i, then calculate the displacement of the node i, y_i, by the equation

$$\mathbf{KY} = \mathbf{F} = [0 \ldots 0\, f_i\, 0 \ldots 0]^T \tag{7}$$

where **K** is the stiffness matrix of the complete catenary system, **Y** is the vector of nodal displacements and **F** is the vector of vertical forces. Thus the stiffness at point i can be obtained. By repeating the same procedure for every node of the contact wire in a span, the stiffness variation in a span is obtained. The calculated results of the two types of catenary system shown in Fig. 2 are presented in Fig. 4 for different catenary tensions. The parameters of the catenary system are quoted from [9]. Graphs 4(a), (b) and (c) show the stiffness variation for the catenary in Fig. 2(a), and graph (d) is the corresponding result for the catenary in Fig. 2(b) when $T_1 = T_2 = 98$ kN. We desire a catenary that has a minimum variation in stiffness, thus for the catenary in Fig. 2(a) the best result is 4(c) and the worst is 4(a). It can also be seen that the heavy compound catenary of Fig. 2(a) is better than the simple catenary of Fig. 2(b). With the preferred heavy compound catenary it can be concluded that the tensions should be reasonably distributed between the catenaries.

3. MODELLING OF THE PANTOGRAPH

A pantograph is a mechanism consisting of two main parts; a steel or aluminium head fitted with a carbon current collector strip is held in contact with the overhead wire by an uplift force which is provided by a spring-loaded or air-operated frame. The air pressure or spring loading provides a nominally constant uplift force to keep the pantograph head and overhead wire in contact. The whole pantograph mechanism is mounted on the roof of a locomotive.

In general, a pantograph incorporates nonlinear damping elements, which include both viscous and coulomb components, and a nonlinear spring [4]. The most widely used model of a pantograph found in the literature, however, is the two DOF linear model shown in Fig. 5(a) and this model is used in this paper. The upper mass, M_1,

represents a pantograph head and the lower mass, M_2, represents the equivalent inertia of the frame. K_1 and C_1 represent the stiffness and damping between the head and the frame respectively, and C_2 represents the damping between the frame and the base. F_1 and F_2 represent the contact force and uplift force, respectively. F_2 is produced by air pressure or spring loading and may be regarded as constant. Furthermore, the two DOF model of the pantograph may be simplified to a SDOF model, as shown in Fig. 5(b), if the stiffness, K_1, is much greater than the stiffness of the contact wire. In Fig. 5(b), $M = M_1 + M_2$ and represents the mass of the whole pantograph including the head and the frame. The difference between the dynamic behaviour of the two DOF and SDOF models will be discussed later in this paper.

4. SDOF TIME-VARYING MODEL OF THE PANTOGRAPH-CATENARY SYSTEM

As mentioned previously, the pantograph and catenary is a coupled (dynamical) system, because they interact with each other through the contact force. The combined system comprises a two DOF model of the pantograph and a continuous stiffness model of the catenary, as shown in Fig. 6(a). This system can be described by a partial linear differential equation with a set of complicated boundary conditions together with two normal linear differential equations.

As the pantograph head moves along with the train, it should maintain contact with the overhead wire. If this is the case then the velocity and acceleration of the pantograph head are related to the local velocity and acceleration of the wire at the contact point, and the deformation and its time derivative at this point. In addition, the acceleration of the pantograph head includes a centripetal acceleration component due to the curvature of the wire. The kinematic relationship at the contact point is described as follows:

$$\frac{dy_p}{dt} = \frac{\partial y}{\partial t} + V\frac{\partial y}{\partial x} \tag{8}$$

$$\frac{d^2y_p}{dt^2} = \frac{\partial^2 y}{\partial t} + 2V\frac{\partial^2 y}{\partial x \partial t} + V^2\frac{\partial^2 y}{\partial x^2} \tag{9}$$

where y_p and y represent the vertical displacement of the pantograph head and contact wire, respectively, V is the operational speed of the train.

Because of these complicated relationships and the associated boundary conditions, it is extremely difficult to obtain an analytical solution to the model in Fig. 6(a). Thus, a simple model without loss of the main dynamic characters of the coupled pantograph-catenary system for the model in Fig. 6(a) needs to be developed. It has been mentioned previously that the stiffness variation of the overhead wire is a source of vibration of the pantograph-catenary system. The stiffness variation in every span is periodically repeated and the nature of this variation has a significant influence on the dynamic performance of the pantograph-catenary system. If we consider the contact wire's static stiffness only and use a SDOF model of the pantograph, the simplest model that has the main dynamic properties of the pantograph-catenary system is shown in Fig. 6(b). If wave propagation in the wire is considered, dynamic rather than static stiffness should be used. The dynamic stiffness of an overhead wire varies with the tension, the density of the wire and the speed of the pantograph. Compared to the static stiffness, the dynamic stiffness will dramatically change when the speed of the pantograph is close to the wave speed in the wire, but it is very similar to the static stiffness if the moving speed is below eighty percent of the wave speed [10]. For simplicity, only the static stiffness of the overhead wire is used in this paper. The differential equation of this model is given by:

$$M\ddot{y} + c\dot{y} + K(t)y = F \tag{10}$$

Omitting the stiffness variation between the droppers, whose effect will be discussed later, and considering a train with constant speed V, then K(t) can be written as

$$K(t) = K_0 + K_s \cos \frac{2\pi V}{L} t \tag{11}$$

where L is the length of a span, and

$$K_0 = \frac{1}{2} (K_{max} + K_{min})$$

$$K_s = \frac{1}{2} (K_{max} - K_{min}) \tag{12 a,b}$$

where K_{max} and K_{min} are the largest and the smallest stiffness in a span, respectively. K_0 can be seen as the average stiffness of the contact wire and K_s is the amplitude of the stiffness fluctuation.

If we set $\omega_n^2 = K_0/M$ and $\omega = 2\pi V/L$, where ω_n is defined as the nominal natural frequency of the pantograph-catenary system and ω is the frequency of the stiffness variation which is related to the train's speed and the length of a span, then equation (10) can be rewritten as

$$\ddot{y} + \frac{C}{M}\dot{y} + \omega_n^2 \left(1 + \frac{K_s}{K_0} \cos \omega t\right) y = \frac{F}{M} \tag{13}$$

This equation can be non-dimensionalised by letting $\tau = \omega_n t$, to give:

$$\frac{d^2y}{d\tau^2} + 2\zeta \frac{dy}{d\tau} + (1 + \alpha \cos r\tau)\, y = f \tag{14}$$

where $2\zeta = \frac{C}{\omega_n M}$, $\alpha = \frac{K_s}{K_0}$, $r = \frac{\omega}{\omega_n} = \frac{2\pi V}{\omega_n L}$ and $f = \frac{F}{K_0}$.

If F is set to zero then equation (14) is the well-known damped Mathieu's equation [11]. Two parameters are very important and determine the dynamic behaviour of the pantograph-catenary system. They are α which represents the stiffness variation of the contact wire, and r which is related to the train's operating speed, the span length and the nominal natural frequency of the pantograph-catenary system. Equation (14) is used in subsequent sections to investigate the pantograph-catenary system's dynamic performance.

5. STABILITY OF THE PANTOGRAPH-CATENARY SYSTEM

In a periodically time-varying system described by (14), the boundaries of stable and unstable regions should be determined first. For a periodically time-varying system $\dot{\mathbf{X}}(t) = \mathbf{A}(t)\,\mathbf{X}(t)$, where $\mathbf{A}(t + T) = \mathbf{A}(t)$ and T is the period, the relationship between $\mathbf{X}(t + T)$ and $\mathbf{X}(t)$ can be written as $\mathbf{X}(t + T) = \mathbf{M}\,\mathbf{X}(t)$. $\mathbf{M}$ is known as the monodromy matrix. According to the Floquet theory the stability of a periodically time-varying system is determined by eigenvalues of its monodromy matrix [12]. For a SDOF system its monodromy matrix and eigenvalues of the monodromy matrix can be obtained numerically by calculating two linear independent solutions of the system's equation under two specified initial conditions during the first period of oscillation [11].

For a practical overhead line system the stiffness uneveness coefficient α is in a range of 0.25 – 0.60, and the highest operational speed of trains is under 500 km per hour, so the coefficient r is less than 1.5. We take a range of 0.2 – 0.7 for α and 0.1 – 2.5 for r and divide this area with a grid whose unit should be small enough to lead to a reasonably accurate solution, and then every crossing point in the grid is calculated by using the 4th order Runge-Kutta method to determine the system's stability at these points.

The results of this calculation are shown in Fig. 7 for three values of damping, $\zeta = 0$, 0.01 and 0.02. Three areas of instability can be seen in Fig. 7 and they occur in regions around r = 0.67, 1 and 2. These areas of instability are dependent upon damping. For example, the system would be unstable for r = 2, $\alpha = 0.25$ and $\zeta = 0$, but would be stable for r = 2, $\alpha = 0.4$ and $\zeta = 0.01$. Since a realistic damping coefficient is generally much greater than those shown in Fig. 7, a practical pantograph-catenary system will probably not suffer from instabilities. Therefore, we can conclude that the loss of contact between the pantograph head and contact wire at higher speeds is probably caused by normal vibration of the pantograph head and not unbounded or unstable vibration. If the stiffness fluctuation between the droppers is considered in equation (14), the plot of stable and unstable regions has few differences from that shown in Fig. 7. The reason for this is that the stiffness variation between the droppers is much smaller than that in a span so the coefficient α, the stiffness variation due to droppers, is very small so it has almost no effect on the stability of the pantograph-catenary system. For simplicity, therefore, the stiffness fluctuation between droppers may be neglected.

6. ANALYTICAL SOLUTION OF DISPLACEMENT AND CONTACT FORCE

Because equation (14) represents a forced parametically-excited system, it is not possible to obtain a closed form solution. However, it is possible to determine an approximate analytical solution using the perturbation method. Fortunately, it is still a linear problem, so the superposition principle can be used. Thus, we can divide the solution into two parts.

$$y = y_t + y_s \tag{15}$$

where y_t and y_s represent the transient and steady-state responses, respectively. It is advisable to use different methods for solutions of y_t and y_s.

6.1 Transient response

The method of multiple scales [11] is used for the solution of the transient response, y_t. We first rewrite equation (14):

$$\ddot{y}_t + 2\,\varepsilon\mu\,\dot{y}_t + (1 + 2\varepsilon\,\cos r\tau)\,y_t = 0 \tag{16}$$

where $2\,\varepsilon = \alpha$ and $\varepsilon\mu = \zeta$, and then take a second-order uniform expansion for y_t of the form,

$$y_t(\tau, \varepsilon) = y_0(T_0, T_1, T_2) + \varepsilon y_1(T_0, T_1, T_2) + \varepsilon^2 y_2(T_0, T_1, T_2) \tag{17}$$

where $T_n = \varepsilon^n\tau$, $n = 0, 1, 2$. Substituting eqn. (17) into eqn. (16) and equating the coefficients of ε^0, ε^1 and ε^2 to zero, we obtain

$$D_0^2\,y_0 + y_0 = 0 \tag{18}$$

$$D_0^2\,y_1 + y_1 = -2\,D_0\,D_1\,y_0 - 2\,\mu D_0\,y_0 - 2y_0\,\cos r\,T_0 \tag{19}$$

$$D_0^2\,y_2 + y_2 = -(D_1^2 + 2D_0\,D_2)\,y_0 - 2\mu D_1 y_0 - 2D_0 D_1 y_1 - 2\mu D_0 y_1 - 2y_1\,\cos \tag{20}$$

where $D_n = \partial^n/\partial T_n$, $n = 0, 1, 2$. If we obtain solutions for equations (18), (19) and (20), and substitute these into equation (17), we obtain

$$y_t = y_0 + \varepsilon y_1 + \varepsilon^2 y_2$$

$$= Ae^{-\zeta\tau}\left\{\cos\left[\left(1-\frac{\zeta^2}{2}-\frac{\varepsilon^2}{4-r^2}\right)\tau+\phi\right]\right.$$

$$+\frac{\varepsilon}{r(2+r)}\cos\left[\left(1-\frac{\zeta^2}{2}+r-\frac{\varepsilon^2}{4-r^2}\right)\tau+\phi\right]$$

$$-\frac{\varepsilon}{r(2-r)}\cos\left[\left(1-\frac{\zeta^2}{2}-r-\frac{\varepsilon^2}{4-r^2}\right)\tau+\phi\right]$$

$$+\frac{\varepsilon^2}{r(2+r)(1+r)}\cos\left[\left(1-\frac{\zeta^2}{2}+2r-\frac{\varepsilon^2}{4-r^2}\right)\tau+\phi\right]$$

$$\left.+\frac{\varepsilon^2}{r(2-r)(1-r)}\cos\left[\left(1-\frac{\zeta^2}{2}-2r-\frac{\varepsilon^2}{4-r^2}\right)\tau+\phi\right]\right\} \qquad (21)$$

A and ϕ are constants decided by the initial conditions of the system. It should be noticed that this solution is only valid when the system is stable.

Equation (21) reveals that transient response consists of some harmonic motions at different frequencies and their amplitudes decay with increasing time due to the negative exponent caused by damping.

6.2 Steady-state response

As the transient response vanishes with increasing time, the steady-state response is the most useful solution to study. To obtain the steady-state response, we rewrite equation (14) as follows:

$$\ddot{y}_s + 2\zeta\dot{y}_s + (1 + \alpha\cos r\tau)\, y_s = f \qquad (22)$$

The solution can be obtained by using the straightforward expansion method [11]. For a better approximate solution of the steady-state response we assume a four term expansion having the form,

$$y_s(\tau, \alpha) = y_0(\tau) + \alpha y_1(\tau) + \alpha^2 y_2(\tau) + \alpha^3 y_3(\tau) \tag{23}$$

Substituting equation (23) into equation (22) and equating coefficients of like powers of α, we obtain

$$\ddot{y}_0 + 2\zeta \dot{y}_0 + y_0 = f \tag{24}$$

$$\ddot{y}_i + 2\zeta \dot{y}_i + y_i = -y_{i-1} \cos r\tau \qquad i = 1, 2, 3 \tag{25}$$

By seeking steady-state responses of equations (24) and (25) successively and substituting them into (23), we obtain

$$y_s = y_0 + \alpha y_1 + \alpha^2 y_2 + \alpha^3 y_3$$

$$= f\left\{1 + \frac{\alpha}{\sqrt{R_1}}\left\{-\cos(r\tau - \phi_1) + \frac{\alpha}{2}\left[\cos\phi_1 + \frac{1}{\sqrt{R_2}}\cos(2r\tau - \phi_1 - \phi_2)\right]\right.\right.$$

$$-\frac{\alpha^2}{4}\left[\frac{2\cos\phi_1}{\sqrt{R_1}}\cos(r\tau - \phi_1) + \frac{1}{\sqrt{R_1}}\left[\frac{1}{\sqrt{R_1}}\cos(r\tau - 2\phi_1 - \phi_2)\right.\right.$$

$$\left.\left.\left.\left.\left.+\frac{1}{\sqrt{R_3}}\cos(3r\tau - \phi_1 - \phi_2 - \phi_3)\right]\right]\right\}\right\} \tag{26}$$

where

$$R_1 = (1 - r^2)^2 + (2\zeta r)^2 \qquad \phi_1 = \tan^{-1}\frac{2\zeta r}{1 - r^2}$$

$$R_2 = (1 - 4r^2)^2 + (4\zeta r)^2 \qquad \phi_2 = \tan^{-1}\frac{4\zeta r}{1 - 4r^2}$$

$$R_3 = (1 - 9r^2)^2 + (6\zeta r)^2 \qquad \phi_3 = \tan^{-1}\frac{6\zeta r}{1 - r^2} \qquad (27a, b, c)$$

Equation (26) shows that the steady-state response of a periodically time-varying system to a *constant external force* is composed of a DC component and some harmonic motions with a dominant component having frequency, r. When the damping is small and r is 1, 1/2 and 1/3, the response is a maximum at these non-dimensional frequencies. They can be regarded as a primary resonance for r equals 1 and sub-resonances for r equals 1/2 or 1/3. This character is very important for a periodically time-varying system, which does not exist in time-invariant systems.

To compare the response predicted by the analytical model described above, it is compared with a numerical solution.

A numerical calculation of the steady-state response was performed using the 4th Runge-Kutta method. It may be used as an exact solution for comparison with the solution given in equation (26), with $\zeta = 0.1$, $\alpha = 0.5$ and $f = 1$. The steady-state peak-to-peak displacements for both methods are plotted in Fig. 7 where it can be seen that the approximate analytical solution is quite satisfactory for the values of r from 0.1 to 1.5.

Using equation (26) some important aspects of the dynamic performance can be predicted, for example, the operation speed causing resonance, the DC component of displacement of the pantograph head and the system's vibration amplitude.

Equations (26) and (27 a,b,c) can be used to show that the stiffness variation between droppers has only a small effect on the system's steady-state response if it is added

into the model. The reason is that a dropper span is much shorter than a whole span, so the coefficient r due to dropper span is much larger than that due to a whole span in terms of the definition of r ($r = 2\pi v/\omega_n L$) for the same operation speed of a train. This will result in large values of R_1, R_2 and R_3, and hence small $1/\sqrt{R_1}$, $1/\sqrt{R_2}$ and $1/\sqrt{R_3}$. In addition, the stiffness variation between the droppers is much smaller than that in a whole span. Therefore, the contribution to the steady-state response due to the stiffness variation within the dropper span is small enough to be neglected.

6.3 Analysis of the pantograph-catenary system's dynamic performance

The results in the normalised form of peak-to-peak, maximum displacement and contact force for a pantograph-catenary system having different parameters are shown in Fig. 9 – Fig. 12 by using equation (26), with setting f = 1. These figures describe main aspects of the pantograph-catenary system's dynamic behaviour which can be summarised as follows:

1. There are three resonance peaks appearing at r = 1/3, 1/2 and approximately 1. The primary resonance is when r is approximately 1 and the others are sub-resonances. For a high speed pantograph-catenary system, for example, the speed at r = 1/3, 1/2 and 1 is about 160, 240 and 480 km/h, and for a standard speed pantograph-catenary system it is about 100, 200 and near 300 km/h, respectively [9].

2. The stiffness variation coefficient α of the contact wire in a single span has a significant influence on the system's dynamic performance because it is the source of the parametrical excitation. It can be seen in Fig. 9 – Fig. 12 that the smaller the coefficient α is, the smaller the variation in the contact force. Therefore, the stiffness variation of the contact wire should be kept as small as

possible. For a heavy compound catenary used for high speed trains, α is about 0.3 and for a simple catenary used for standard speed trains α is about 0.6. Thus the compound system is clearly preferable, but it would of course be much more costly.

3. When the peak-to-peak contact force or displacement is greater than the maximum contact force or displacement, loss of contact between the pantograph head and contact wire will occur. Thus, the first cross-over point on the peak-to-peak and maximum contact force graphs represents an upper limit of the operational speed of trains. For a heavy compound catenary the highest operational speed is mainly limited by the primary resonance, and for a simple catenary the highest operation speed is mainly limited by the lowest sub-resonance.

4. The damping between the pantograph's frame and head has an important effect on the shape of the graphs around resonance; the smaller the damping, the sharper the resonance. A small increase in damping will increase the margin of positive contact force or raise the upper operational speed of the train.

5. Increasing the average stiffness of the contact wire and decreasing the mass of the pantograph both have a positive effect on improving the pantograph-catenary system's performance since this will raise the system's nominal natural frequency which will lead to a reduction in the value of r for the same operational speed, or allow a higher speed for the same value of r.

7. TWO DOF TIME-VARYING MODEL OF A PANTOGRAPH-CATENARY SYSTEM

A two DOF model of the pantograph-catenary system is shown in Fig. 13, where M_1, K_1 and C_1 represent the mass, stiffness and damping of the pantograph head, respectively, and M_2 and C_2 represent the mass and dampng of the pantograph frame, respectively. K(t) represents the stiffness of the contact wire and F is a constant uplift force. A specific pantograph-catenary system from [9] has the following parameters: $M_1 = 6.5$ kg, $M_2 = 8.5$ kg, $K_1 = 39000$ N/m, $C_1 = 120$ Ns/m, $C_2 = 30$ Ns/m, F = 54 N and L = 50 m. K_{max} and K_{min} are calculated by using FEM developed in this paper, and their values are: $K_{max} = 5730$ N/m and $K_{min} = 2920$ N/m. The steady-state response of the system is calculated by using the 4th order Runge-Kutta method at an operational speed, V = 300 km/h. A comparison of the results of the SDOF model in terms of displacements is shown in Fig. 14. It can be seen from Fig. 14(a) that there is almost no difference between the two DOF model and SDOF model in terms of the displacement of the pantograph head. As to the displacement of the pantograph frame, the difference between the two models is a DC shift in the frame displacement. This DC shift can be regarded as the static displacement of the pantograph frame.

The larger the stiffness is between the head and frame, the smaller the static displacement of the frame. For a SDOF model the connection between M_1 and M_2 is rigid, so the static displacement of the frame is the smallest. By using a two DOF model of the pantograph-catenary system, the influences of the pantograph head's mass, damping and stiffness on the system's dynamic performance can also be investigated. The results of changing mass and stiffness can be seen in Fig. 15 and Fig. 16, respectively. Some important conclusions may be stated as follows:

1. For a given speed, reducing either the head mass or frame mass will marginally decrease the contact force fluctuation between the pantograph head and contact wire. The main function of reducing mass is to increase the system's nominal natural frequency and thus allow a higher operational speed for the same variation in contact force.

2. Decreasing the stiffness between the head and the frame can reduce the sharpness of the resonance, and thus reduce the variation in the contact force. The reason for this is that a softer spring is a better absorber of an impulsive force.

3. Changing the damping between the pantograph head and frame has almost no effect on the contact force. Setting C_1 = 80, 120 and 160 Ns/m, the results overlay and so they are not plotted.

8. CONCLUSIONS

A periodically time-varying SDOF model of the pantograph-catenary system has been developed for the analytical study of the system's dynamics. It is simple but retains the main dynamic properties of the system. Although there is the possibility of a stability problem for a periodically time-varying system, typical pantograph-catenary systems operate in a stable region when their operating speeds are limited to under 500 km/h and there is a small amount of damping present. The loss of contact between the pantograph head and contact wire at higher speeds, therefore, is due to bounded vibration. The stiffness variation between the catenary spans is the initial source of a parametrical excitation causing vibrations of the pantograph-catenary system during the train's operation.

Below the speed of about 500 km/h there are three bounded resonance areas for the pantograph-catenary system which limit the highest operation speed of trains. The stiffness variation coefficient of the catenary and the damping between the pantograph frame and base affect the shape of the resonant response significantly. For a heavy compound catenary its stiffness variation coefficient is smaller, so the upper limit of operation speed is limited by the primary resonance and thus a higher speed is possible. On the other hand, for a simple catenary its stiffness variation coefficient is larger, so the upper limit of operation speed is limited by the first subresonance area and thus there is a lower speed limit. Changing the average stiffness of the catenary and the mass of the pantograph will lead to a change in the nominal natural frequency of the pantograph-catenary system and thus the upper limit of the train's operational speed.

As mentioned in the introduction, the influence of wave propagation in the overhead wire has not been included in the model discussed in this paper. If wave propagation is considered, the dynamic rather than static stiffness should be used. Because the dynamic stiffness fluctuation will become larger than the static stiffness fluctuation when the operational speed of a train is close to the wave speed in the wire, the dynamic performance of the pantograph-catenary system at higher speeds will be worse than that predicted by the model used in this paper.

9. REFERENCES

[1] Ockenden, J.R. and Taylor, A.B. The dynamics of a current collection system for an electric locomotive. Proceedings of the Royal Society of London, Series A 322 (1971), 447-468.

[2] Vinayagalingam, T. Computer evaluation of controlled pantographs for current collection from simple catenary overhead equipment at high speed.

ASME Journal of Dynamics Systems, Measurement, and Control, 105 (1983), 287-294.

[3] Wormly, D., Seering, W., Eppinger, S. and O'Connor, D. Dynamic performance characteristics of new configuration pantograph-catenary systems. Report No. DOT/OST/P34-85/023, US Department of Transportation, October 1984.

[4] Seering, W., Ambruster, K., Vesely, C. and Wormly, D. Experimental and analytical study of pantograph dynamics. Journal of Dynamics Systems, Measurement and Control, 113 (1991), 242-247.

[5] Wu, T.X. Analysis and calculation of catenary by FEM. Journal of the China Railway Society, 18 June (1996), 44-49 (in Chinese).

[6] Wu, T.X. Study of current collection from catenary-pantograph at high speed by simulation. Journal of the China Railway Society, 18 Aug (1996), 55-61 (in Chinese).

[7] Manabe, K. Periodical dynamic stabilities of a catenary-pantograph system. Quarterly Report of RTRI 35 (1994), 112-117.

[8] Yagi, T., Stensson, A. and Hardell, C. Simulation and visualisation of the dynamic behaviour of an overhead power system with contact breaking. Vehicle System Dynamics, 25 (1996), 31-49.

[9] Manabe, K. and Fujii, Y. Overhead system resonance with multi-pantographs and countermeasures. Quarterly Report of RTRI 30 (1989), 175-180.

[10] Lesser, M., Karlsson, L. and Drugge, L. An interactive model of a pantograph-catenary system. Vehicle System Dynamics, Supplement 25 (1996), 397-412.

[11] Nayfeh, A. Nonlinear oscillations. John Wiley (1979).

[12] Ibrahim, R. and Barr, A. Parametric vibration, Part 1: Mechanics of linear problems. Shock and Vibration Digest, 10(1), (1978), 15-29.

[13] Richards, J. Analysis of Periodically Time-varying Systems. Springer-Verlag (1983).

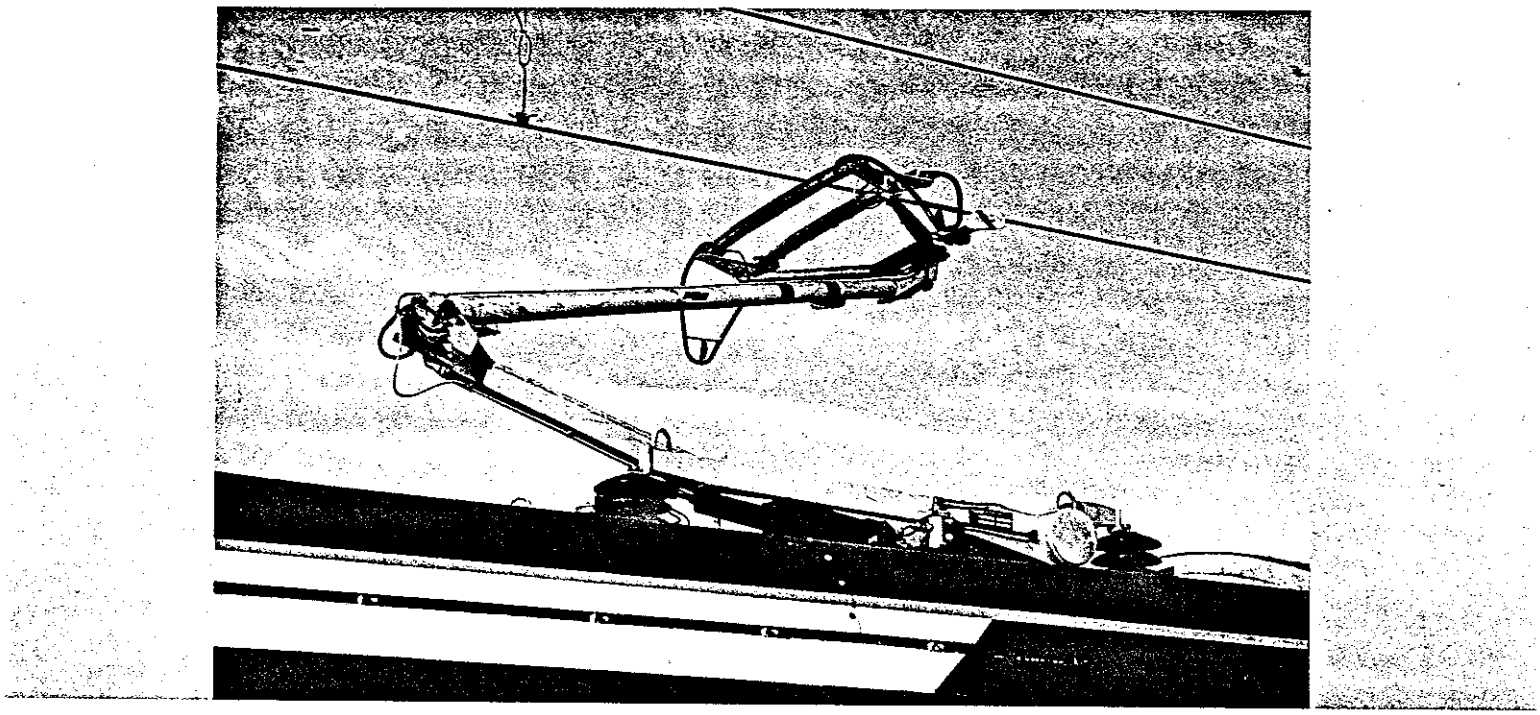

Figure 1 Pantograph and overhead wire.

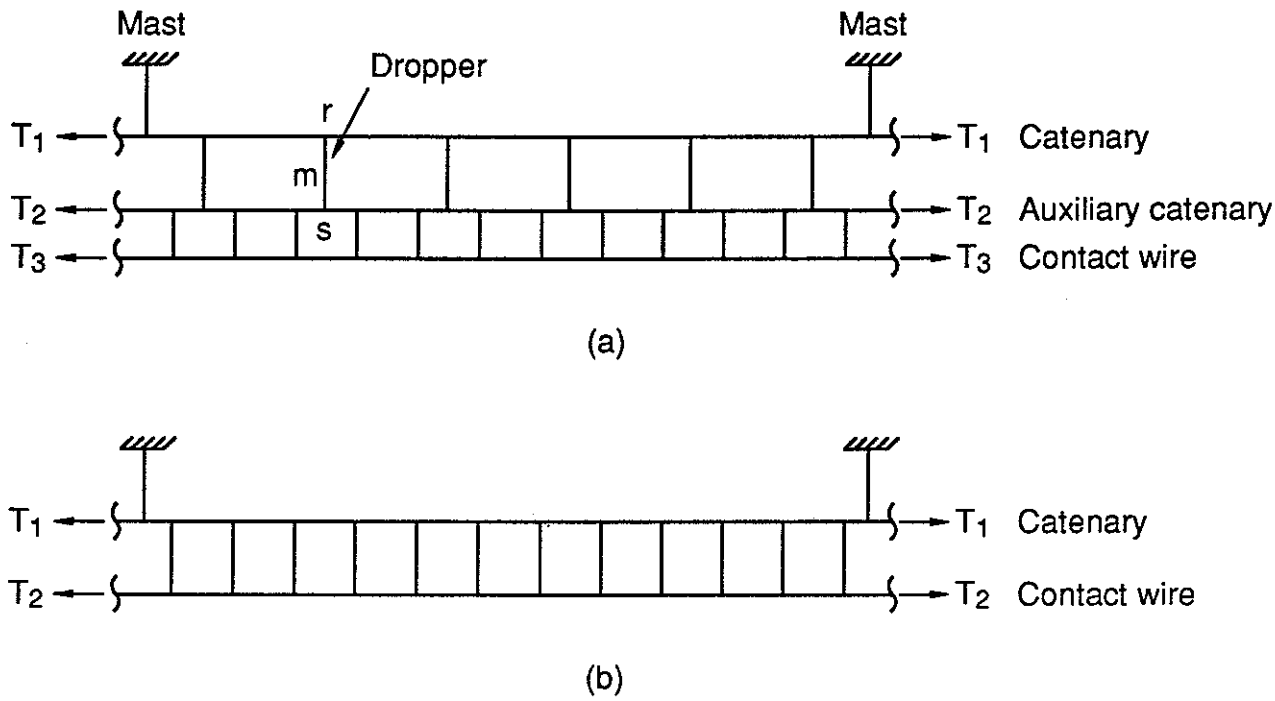

Figure 2 Catenary system. (a) Heavy compound catenary. (b) Simple catenary.

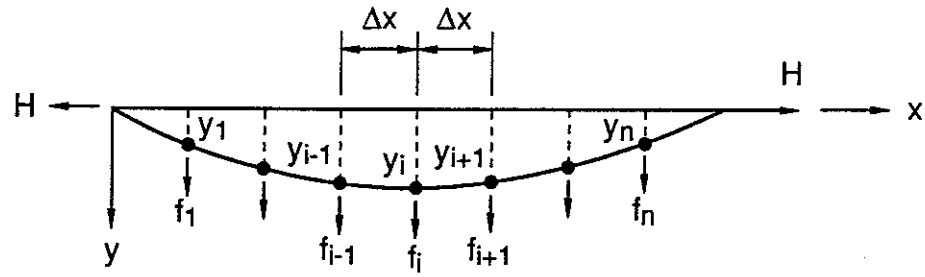

Figure 3 Discretization of catenary.

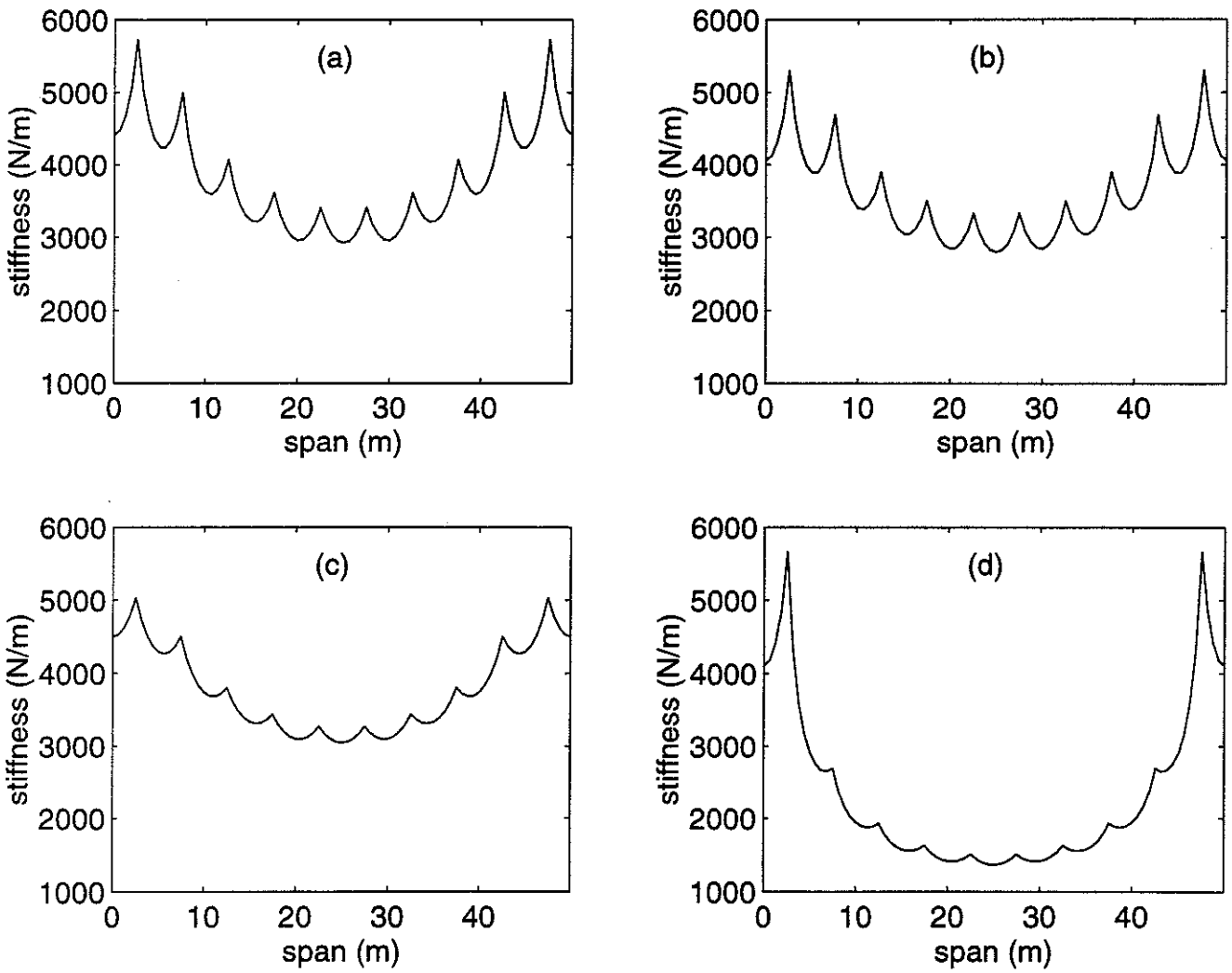

Figure 4 Stiffness of contact wire in a span: (a) $T_1 = 24.5$ kN, $T_2 = T_3 = 14.7$ kN; (b) $T_1 = T_3 = 14.7$ kN, $T_2 = 24.5$ kN; (c) $T_1 = T_2 = 14.7$ kN, $T_3 = 24.5$ kN; (d) $T_1 = T_2 = 9.8$ kN.

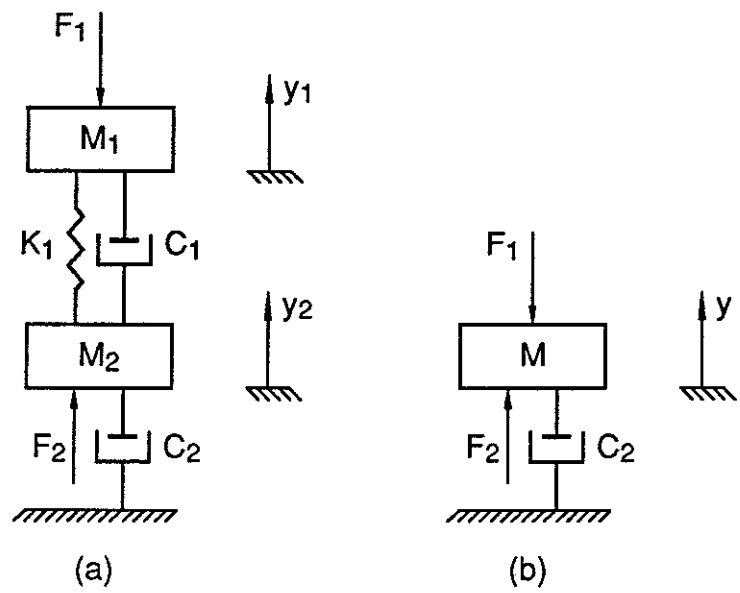

Figure 5 Pantograph model.

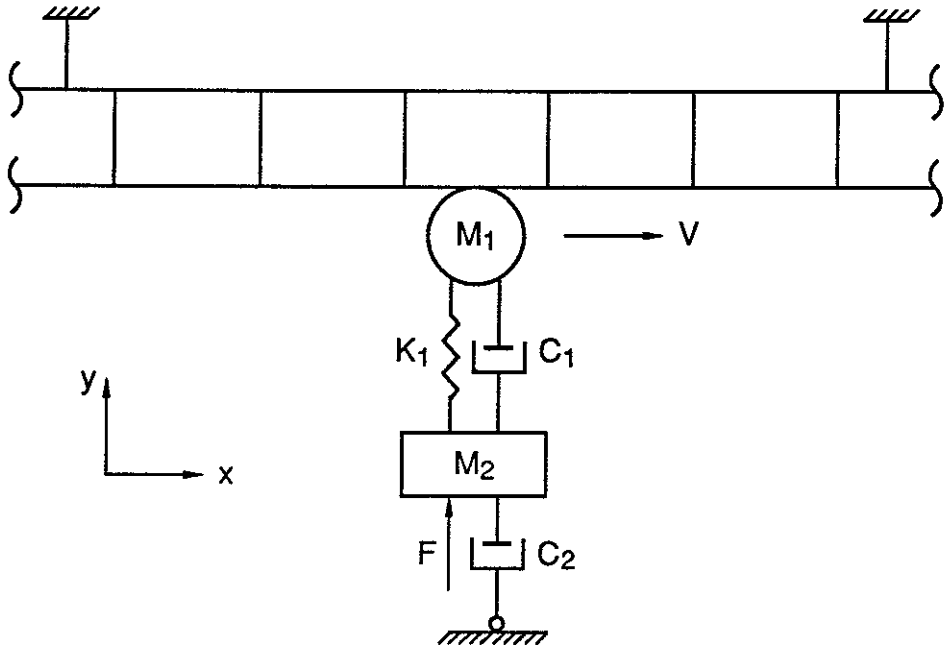

(a)

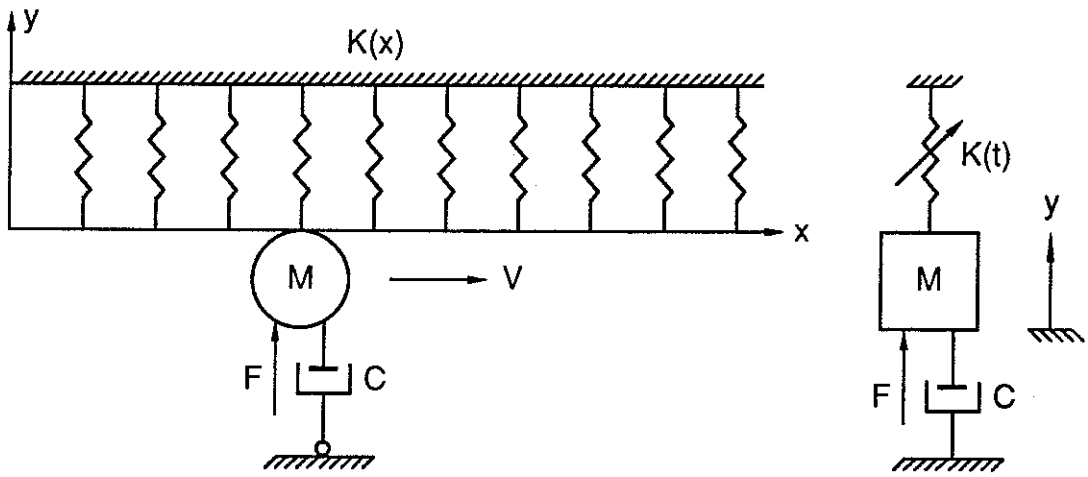

(b)

Figure 6 Model of pantograph - catenary system.

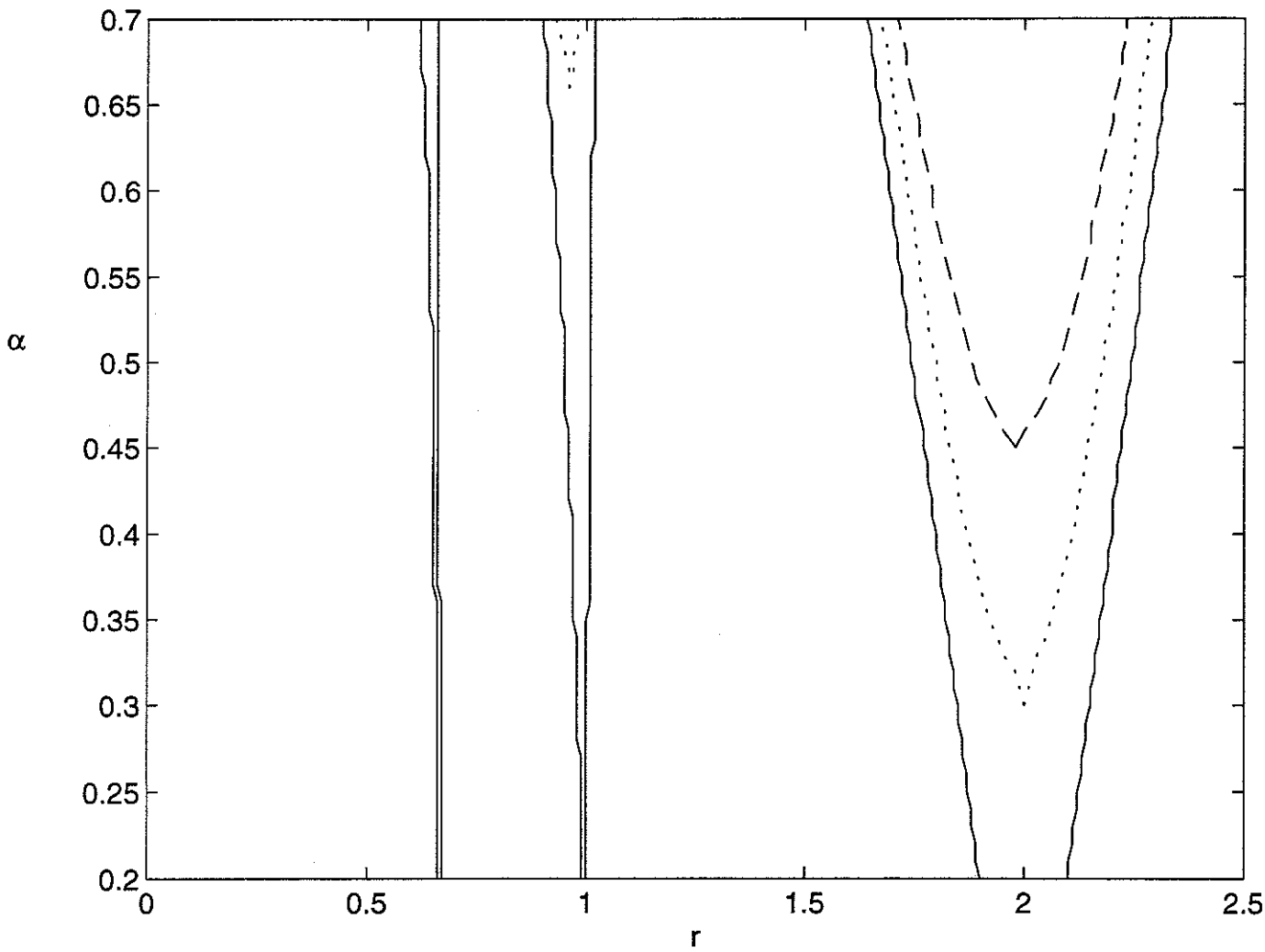

Figure 7 Stable and unstable regions of pantograph-catenary system: —— $\zeta = 0$; ····· $\zeta = 0.01$; – – – $\zeta = 0.02$.

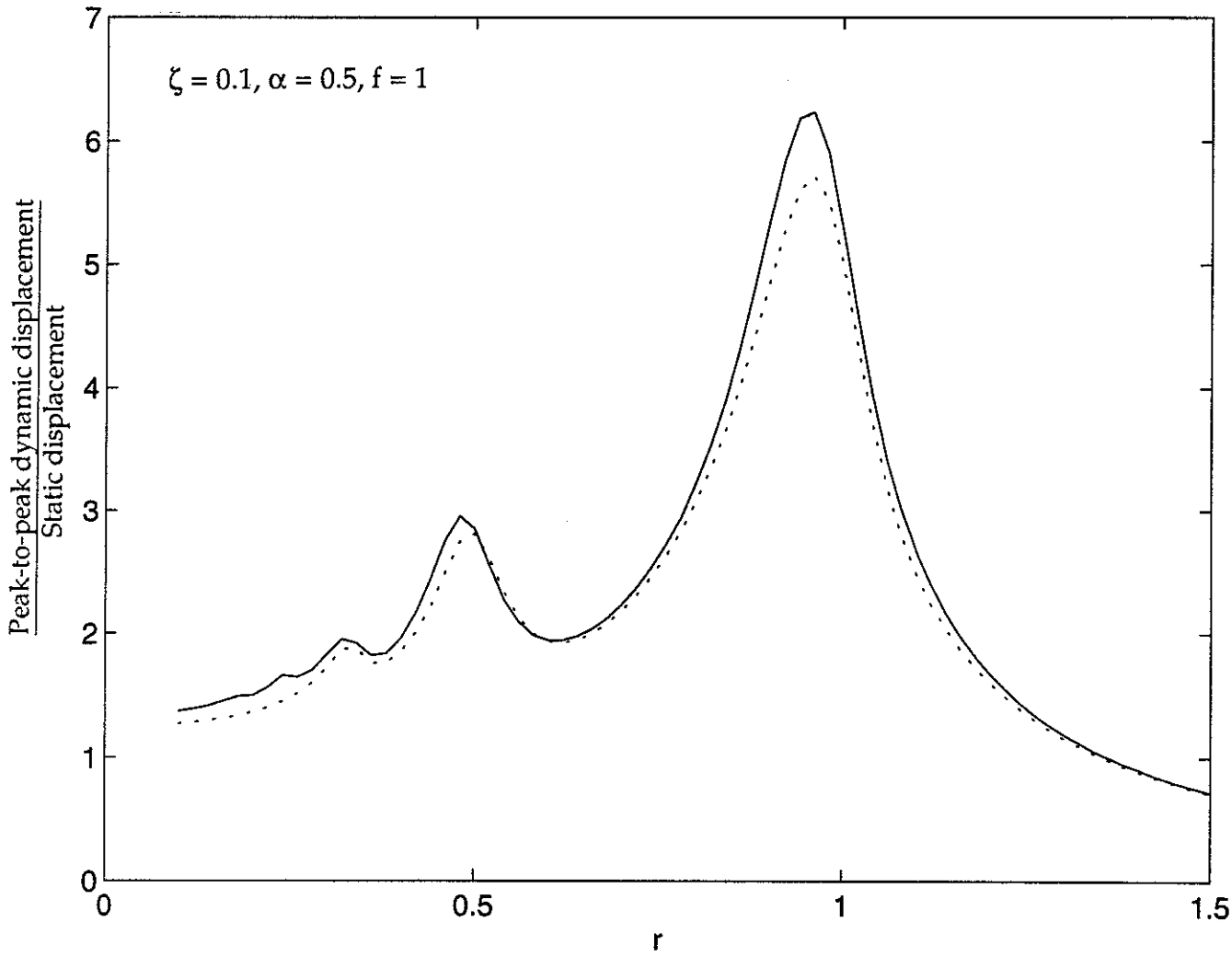

Figure 8 Comparison between solutions by numerical method and perturbation method: — the 4th Runge-Kutta method; ····· perturbation method.

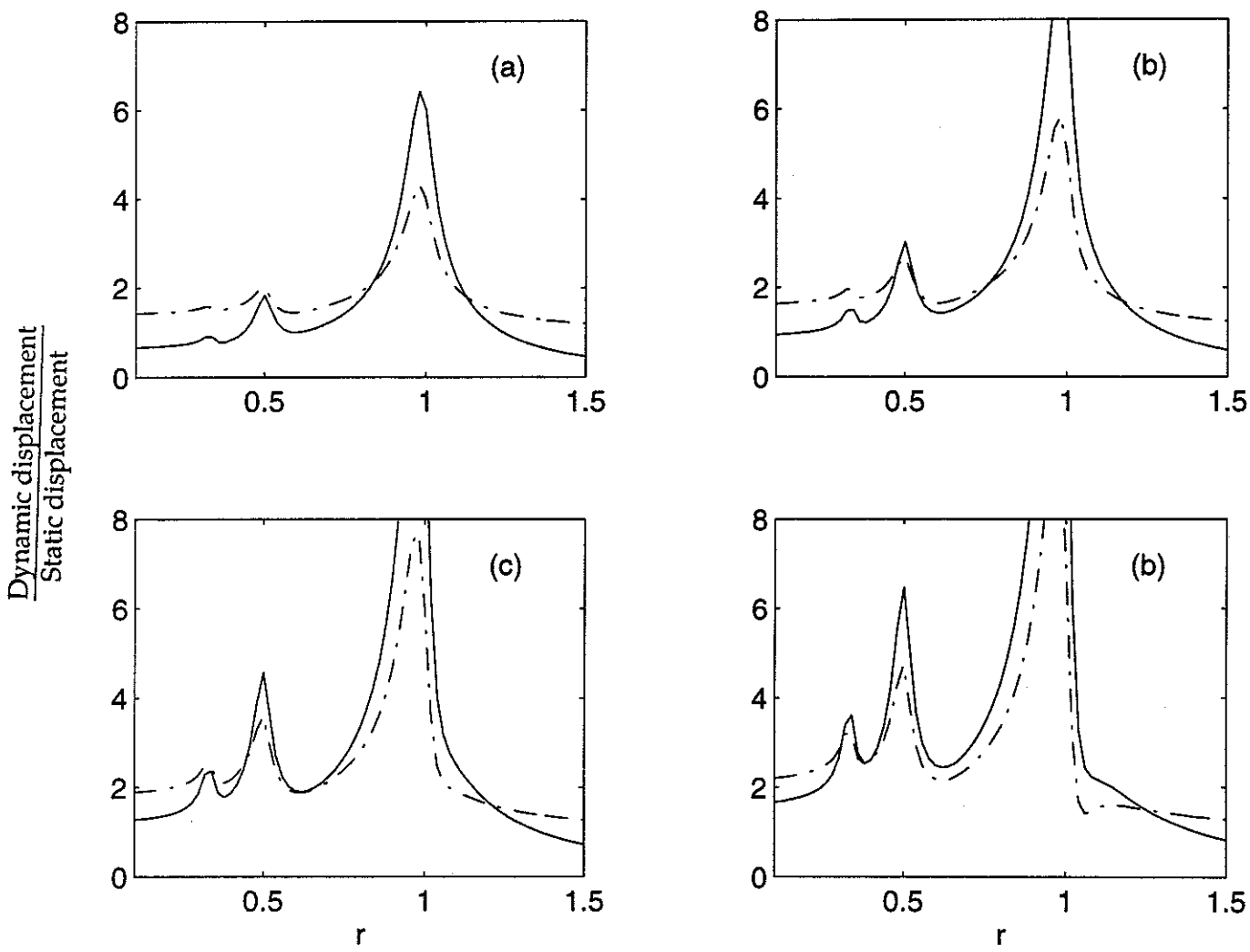

Figure 9 Peak-to-peak and maximum normalised displacement, $\zeta = 0.05$ and $f = 1$:
— peak-to-peak displacement; – · – · maximum displacement.
(a) $\alpha = 0.3$, (b) $\alpha = 0.4$, (c) $\alpha = 0.5$, (d) $\alpha = 0.6$.

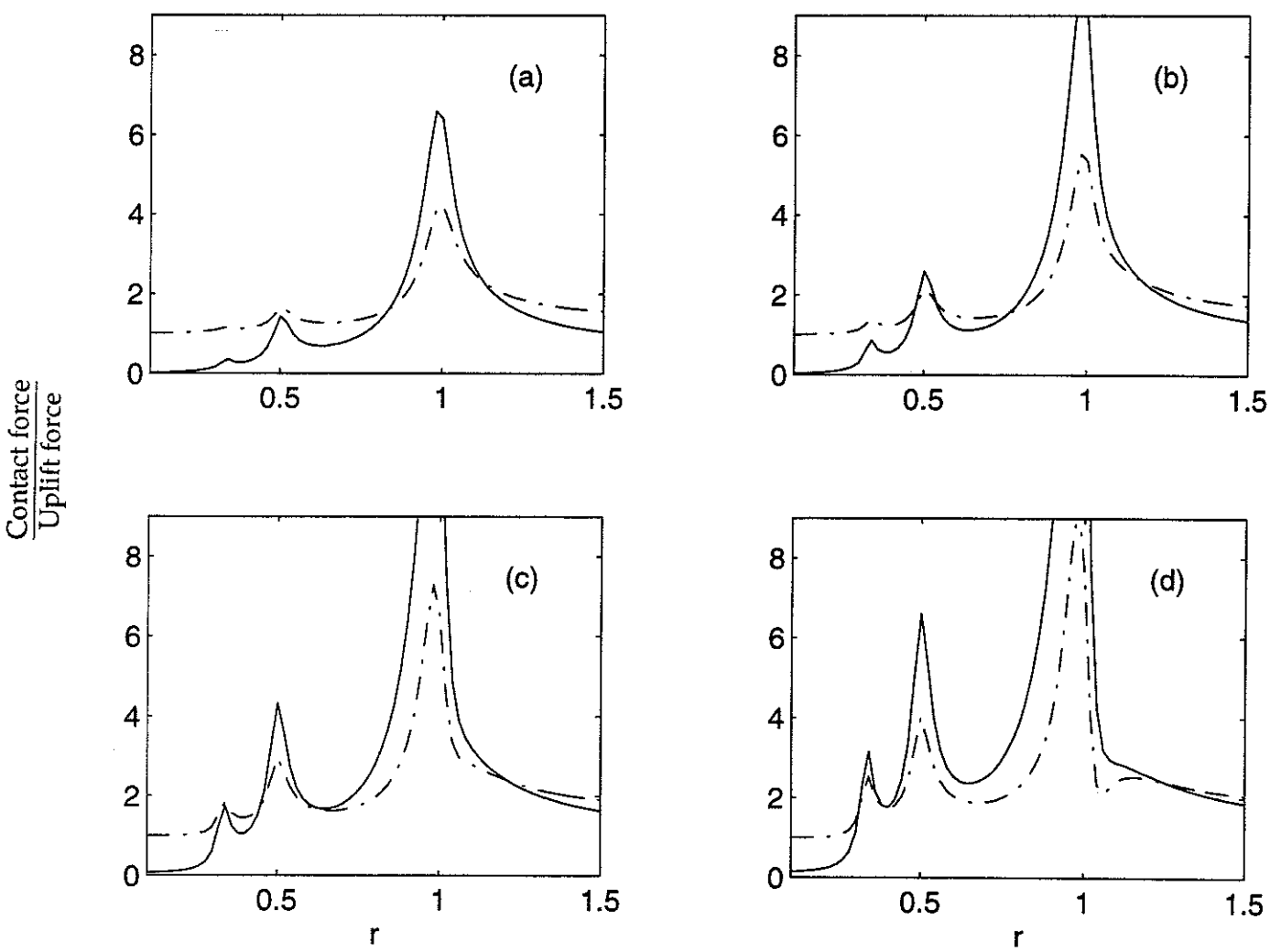

Figure 10 Peak-to-peak and maximum normalised contact force, $\zeta = 0.05$ and $f = 1$:
—— peak-to-peak contact force; – · – · maximum contact force.
(a) $\alpha = 0.3$, (b) $\alpha = 0.4$, (c) $\alpha = 0.5$, (d) $\alpha = 0.6$.

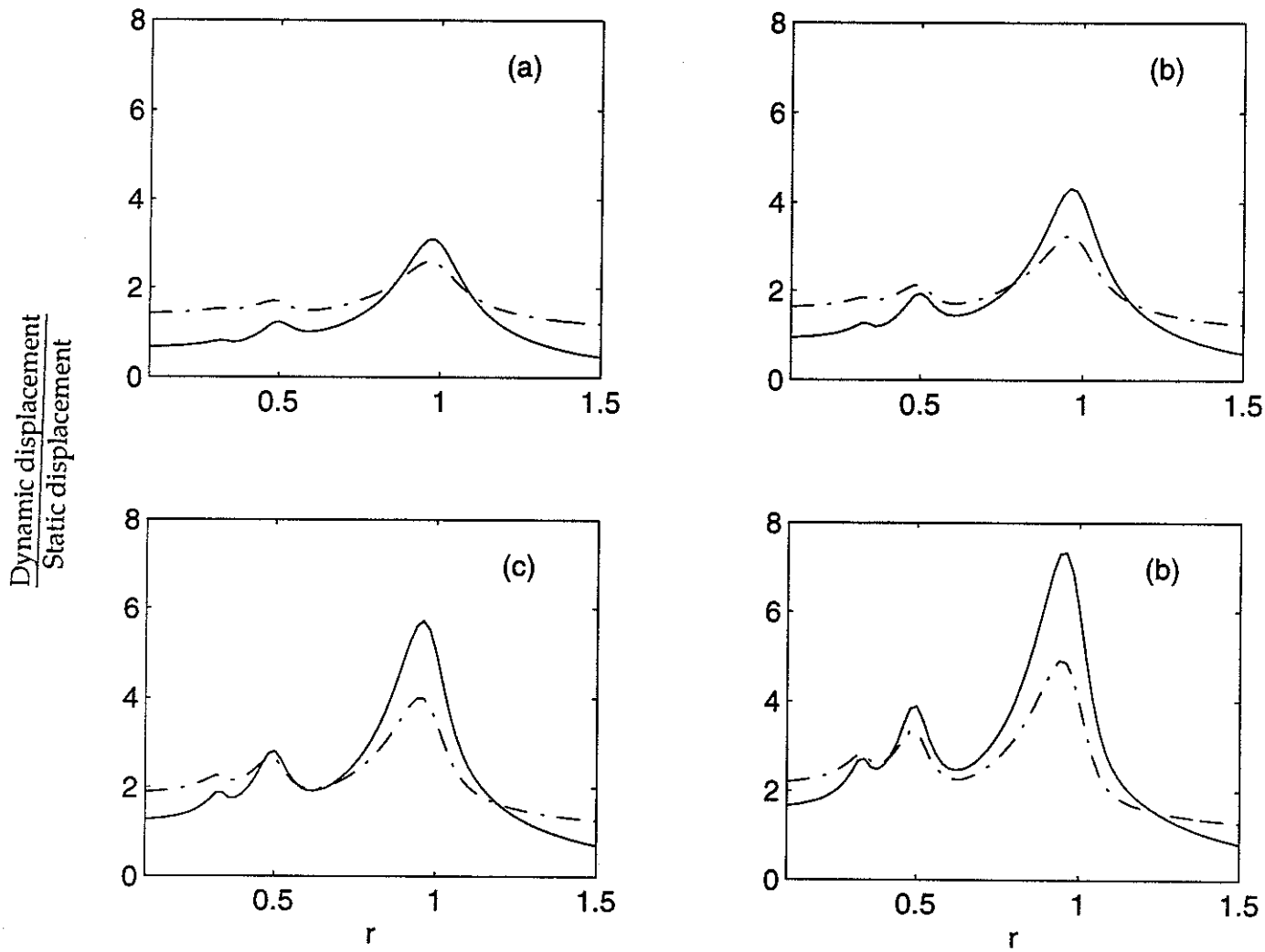

Figure 11 Peak-to-peak and maximum normalised displacement, $\zeta = 0.1$ and $f = 1$:
—— peak-to-peak displacement; – · – · maximum displacement.
(a) $\alpha = 0.3$, (b) $\alpha = 0.4$, (c) $\alpha = 0.5$, (d) $\alpha = 0.6$.

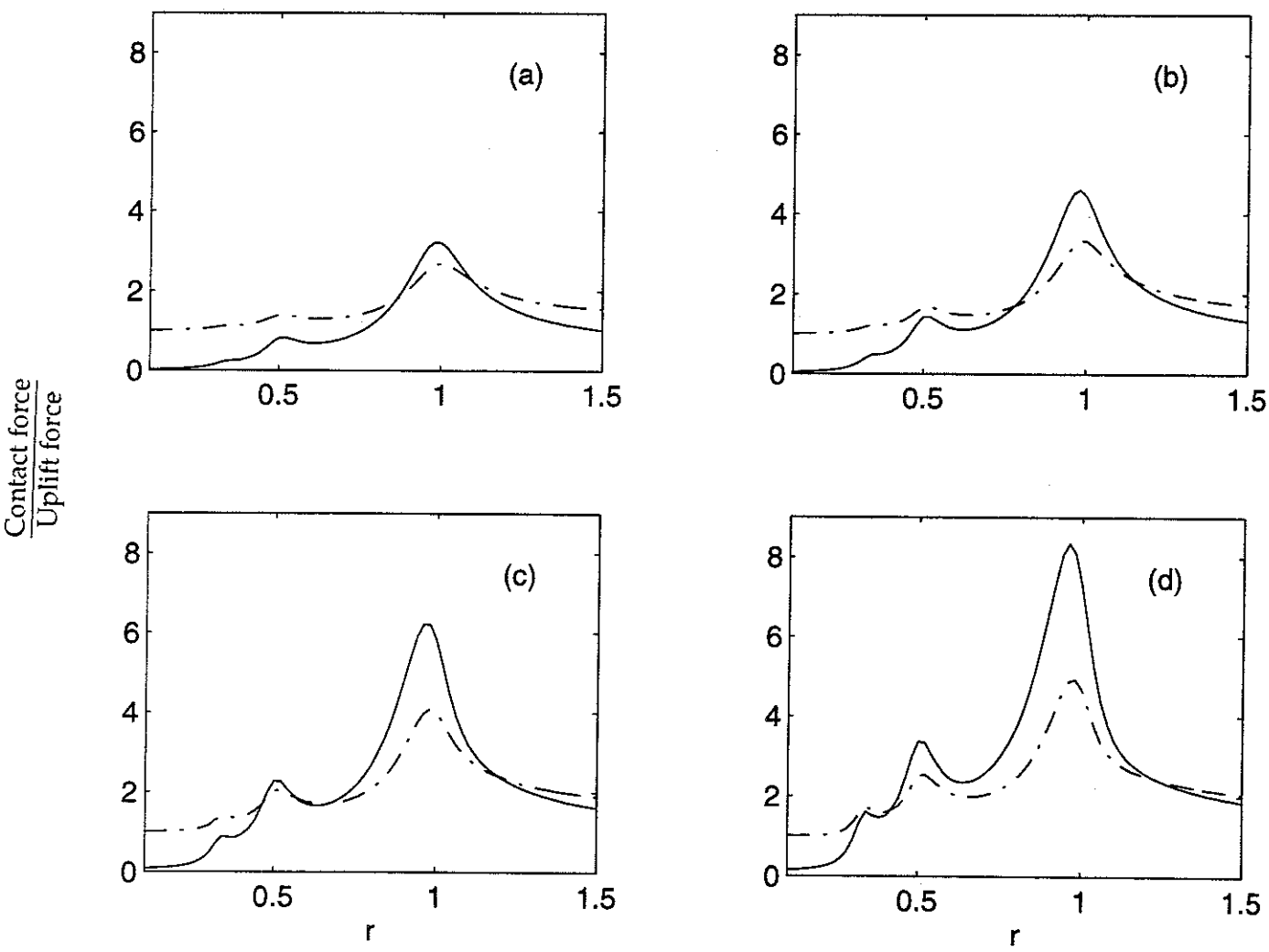

Figure 12 Peak-to-peak and maximum normalised contact force, $\zeta = 0.1$ and $f = 1$:
— peak-to-peak contact force; – · – · maximum contact force.
(a) $\alpha = 0.3$, (b) $\alpha = 0.4$, (c) $\alpha = 0.5$, (d) $\alpha = 0.6$.

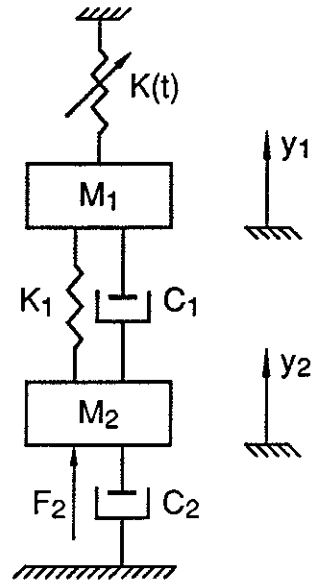

Figure 13 Two DOF model of pantograph - catenary system.

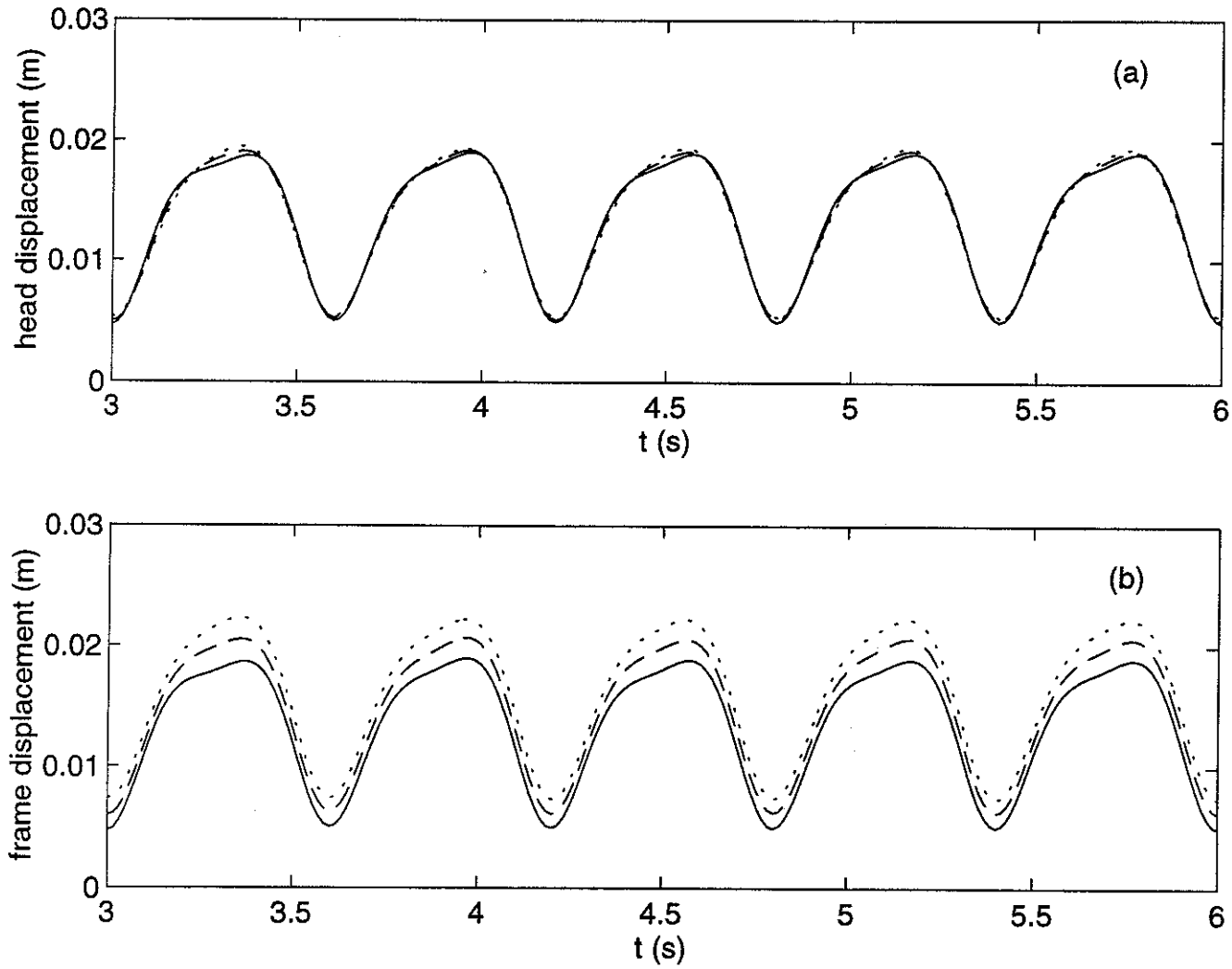

Figure 14 Comparison of the steady-state response from the two DOF model and SDOF model at v = 300 km/h: — SDOF model; – – – two DOF model with K_1 = 39 kN/m; ····· two DOF model with K_1 = 20 kN/m.

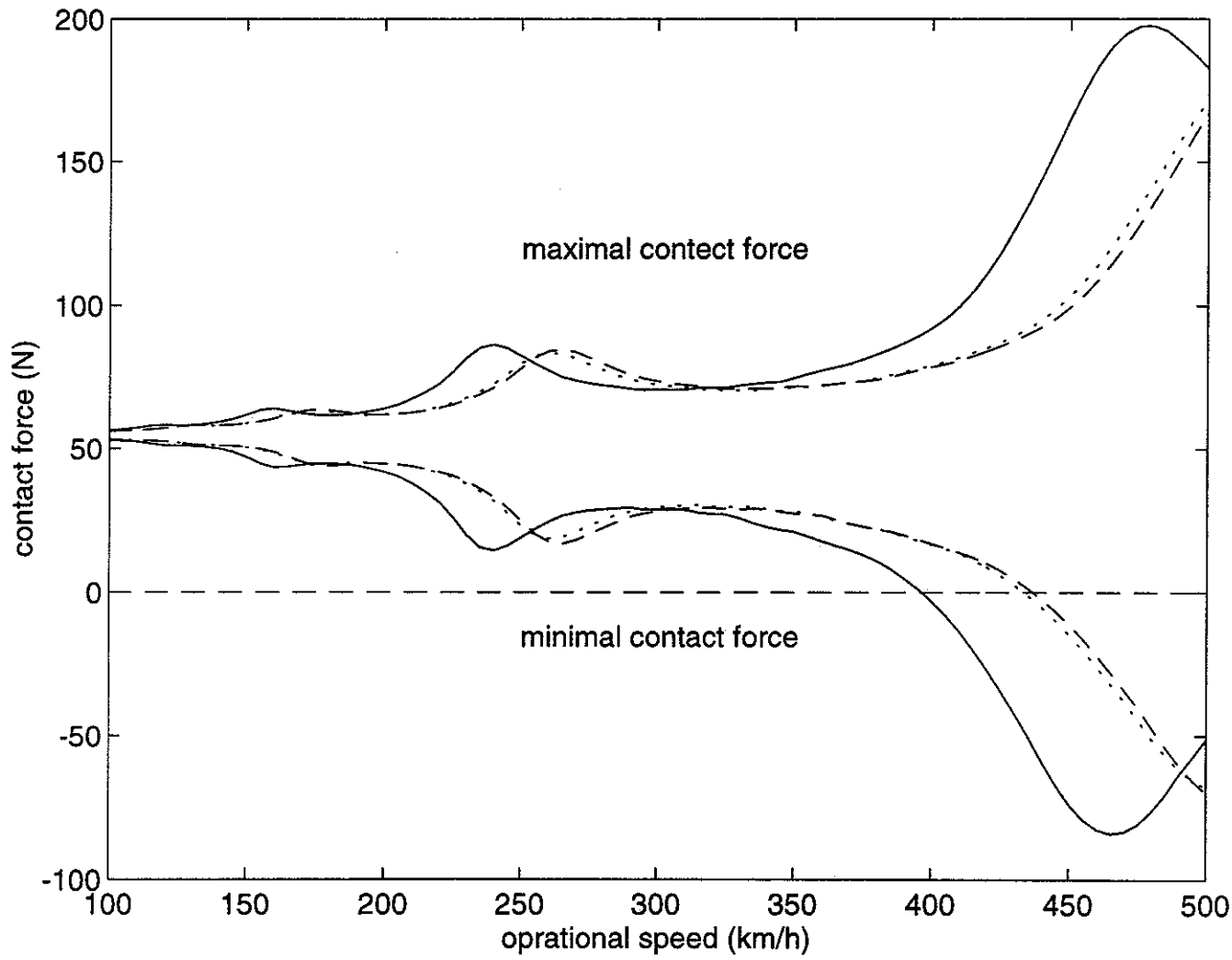

Figure 15 Influences of different mass with $K_1 = 39$ kN/m, $C_1 = 120$ Ns/m and $C_2 = 30$ Ns/m: — $M_1 = 6.5$ kg, $M_2 = 8.5$ kg, ····· $M_1 = 4.0$ kg, $M_2 = 8.5$ kg, – – – $M_1 = 6.5$ kg, $M_2 = 6.0$ kg.

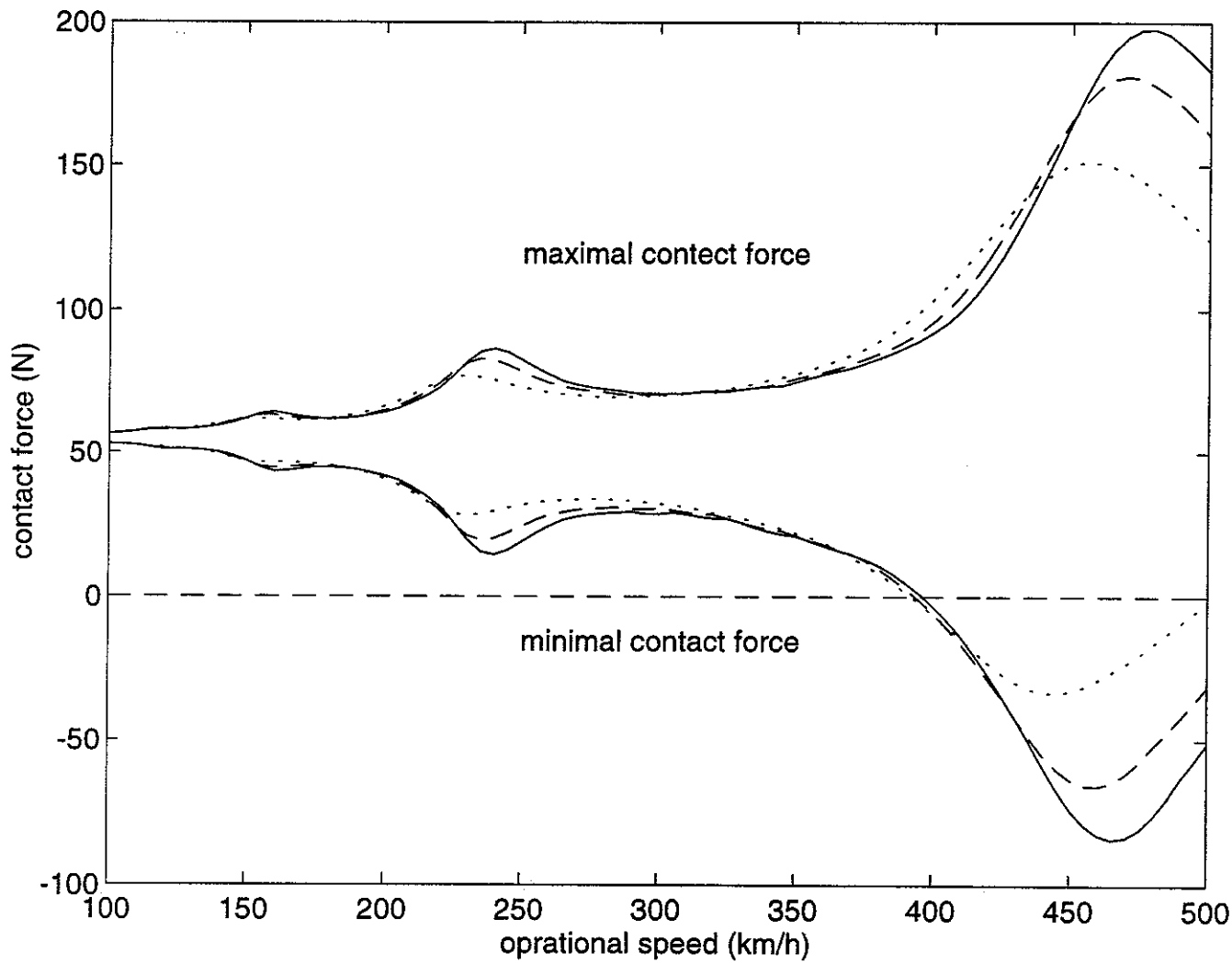

Figure 16 Influences of different stiffness between head and frame with $M_1 = 6.5$ kg, $M_2 = 8.5$ kg, $C_1 = 120$ Ns/m and $C_2 = 30$ Ns/m:
— $K_1 = 39$ kN/m, – – – $K_1 = 20$ kN/m, ····· $K_1 = 10$ kN/m.